



# Vibration analysis of rectangular plates with general elastic boundary supports

W.L. Li\*

*United Technologies Research Center, 411 Silver Lane, East Hartford, CT 06108, USA*

Received 22 October 2002; accepted 28 April 2003

---

## Abstract

In this investigation, the Rayleigh–Ritz method is used to determine the modal characteristics of a rectangular plate with general elastic supports along its edges. Each of the admissible functions here is composed of a trigonometric function and an arbitrary continuous function that is introduced to ensure the sufficient smoothness of the so-called residual displacement function at the edges. As a result, a drastic improvement of the convergence can be expected of the solution expressed as a series expansion in terms of the admissible functions. Perhaps more importantly, this study has developed a general approach for deriving a complete set of admissible functions that can be universally applied to various boundary conditions. Several numerical examples are given to demonstrate the accuracy and convergence of the current solution.

© 2003 Elsevier Ltd. All rights reserved.

---

## 1. Introduction

Vibrations of rectangular plates with various boundary conditions have been extensively investigated for many years. The related publications can be counted in thousands [1]. This potentially gives rise to a problem that one may be easily inundated by the abundance of the available techniques or choices. In addition, a literature survey reveals that most previous investigations have mostly dealt with a scheme or technique that is only suitable for a particular type of boundary conditions. It is well known that the exact solutions are generally available only for plates that are simply supported along at least one pair of opposite edges. For other boundary conditions, however, one may have to use approximate methods such as the Rayleigh–Ritz method.

---

\*Tel.: +1-860-610-7640; fax: +1-860-610-7134.

*E-mail address:* [liw@utrc.utc.com](mailto:liw@utrc.utc.com) (W.L. Li).

The selection of appropriate admissible functions is of critical importance in the Rayleigh–Ritz method because the accuracy of the solution will usually depend upon how well the actual displacement can be faithfully represented by them. In practice, the displacement of a plate is often expanded in terms of the characteristic functions for beams with the similar boundary conditions [2–5]. Although the beam functions are generally known in the forms of the trigonometric and hyperbolic functions, they contain some integration and frequency parameters that are dependent upon boundary conditions. Consequently, there requires a specific set of characteristic functions for each type of boundary conditions. However, just considering the four simplest homogeneous cases (i.e., simply supported, clamped, free and guided), one should realize that they can constitute 55 different boundary conditions for a rectangular plate. Thus, the use of beam functions is still a very tedious process. This problem will become much more serious for plates that are elastically restrained along its edges. This is probably the reason why the previous investigations have been mostly focused on the problems that involve some kind of simplifications with respect to the arrangement of elastic restraints [6–10].

Instead of the beam functions, one can also use other forms of admissible functions such as simple or orthogonal polynomials, trigonometric functions and their combinations [11–20]. When using only lower order polynomials, since they do not form a complete set, the solution becomes less definitive in regard to its convergence. A well-known problem arises with use of a complete set of orthogonal polynomials, that is, the higher order polynomials tend to become numerically unstable due to the computer round-off errors [16]. Although a Fourier series representation may be able to avoid these difficulties, it is usually only applicable to some very simple boundary conditions. In Ref. [17], a set of static beam functions was used to determine the natural frequencies of elastically restrained plates. As indicated by the name, the static beam functions represent the general solutions of a beam under a series of static sinusoidal loads distributed along the length of the beam. Mathematically, each of the static beam functions consists of a sine or cosine function (the particular solution) and a polynomial function of no more than third order (the general solution). The coefficients of the polynomials need to be calculated from boundary conditions. Making use of the Stokes's transformation, Wang et al. [18,19] have extended the Fourier series solution to other, more complicated, boundary conditions than the simply supported. The key result there is that the derivatives of the series expansion cannot be simply obtained through term-by-term differentiation due to the possible discontinuities at the boundaries. Although such a technique has mathematically corrected a common mistake in finding the derivatives of a Fourier series, it does not provide a remedy to the slow-convergence problem that may have actually limited the extension of the Fourier solution to other boundary conditions. Recently, Li [21] proposed an improved Fourier series method in which the beam displacement is expanded into a Fourier cosine series plus an auxiliary polynomial function. Unlike in the previous studies, however, the polynomial function is simply used there for improving the smoothness of the residual displacement function at the end points, rather than satisfying a particular boundary condition. As a result, not only is it always possible to expand the displacement in a Fourier series for beams with any boundary conditions, but also the solution is remarkably improved with respect to both of its accuracy and convergence. The convergence of the solution can be further improved if a different discretization scheme based on the Galerkin method, instead of the Fourier method, is employed in solving the governing differential equation [22]. The convergence of the sine and cosine series expansions is investigated in Ref. [23] and it is

shown that the cosine series expression typically converges faster for beams under general elastic supports. This Fourier series method has been extended to plates that are simply supported along a pair of opposite edges and elastically restrained along the others [24]. The admissible functions used there exactly satisfy the plate, rather than beam, boundary conditions along all edges.

## 2. Vibration analysis of rectangular plates

The governing differential equation for the free vibration of a plate is given by

$$D\nabla^4 w(x, y) - \rho h \omega^2 w(x, y) = 0, \tag{1}$$

where  $\nabla^4 = \partial^4/\partial x^4 + 2\partial^4/\partial x^2\partial y^2 + \partial^4/\partial y^4$ ,  $w(x, y)$  is the flexural displacement,  $\omega$  is angular frequency, and  $D, \rho$  and  $h$  are, respectively, the flexural rigidity, the mass density and the thickness of the plate (a list of symbols is given in Appendix A).

In terms of the flexural displacement, the bending and twisting moments and transverse shearing forces can be expressed as

$$M_x = -D \left( \frac{\partial^2 w}{\partial x^2} + \nu \frac{\partial^2 w}{\partial y^2} \right), \tag{2}$$

$$M_y = -D \left( \frac{\partial^2 w}{\partial y^2} + \nu \frac{\partial^2 w}{\partial x^2} \right), \tag{3}$$

$$M_{xy} = -D(1 - \nu) \frac{\partial^2 w}{\partial x \partial y}, \tag{4}$$

$$Q_x = -D \frac{\partial}{\partial x} (\nabla^2 w) + \frac{\partial M_{xy}}{\partial y} = -D \left( \frac{\partial^3 w}{\partial x^3} + (2 - \nu) \frac{\partial^3 w}{\partial x \partial y^2} \right) \tag{5}$$

and

$$Q_y = -D \frac{\partial}{\partial y} (\nabla^2 w) + \frac{\partial M_{xy}}{\partial x} = -D \left( \frac{\partial^3 w}{\partial y^3} + (2 - \nu) \frac{\partial^3 w}{\partial x^2 \partial y} \right). \tag{6}$$

The boundary conditions for an elastically restrained rectangular plate are

$$k_{x0} w = Q_x, \quad K_{x0} \partial w / \partial x = -M_x, \quad \text{at } x = 0, \tag{7, 8}$$

$$k_{x1} w = -Q_x, \quad K_{x1} \partial w / \partial x = M_x, \quad \text{at } x = a, \tag{9, 10}$$

$$k_{y0} w = Q_y, \quad K_{y0} \partial w / \partial y = -M_y, \quad \text{at } y = 0 \tag{11, 12}$$

and

$$k_{y1} w = -Q_y, \quad K_{y1} \partial w / \partial y = M_y, \quad \text{at } y = b, \tag{13, 14}$$

where  $k_{x0}$  and  $k_{x1}$  ( $k_{y0}$  and  $k_{y1}$ ) are the linear spring constants, and  $K_{x0}$  and  $K_{x1}$  ( $K_{y0}$  and  $K_{y1}$ ) are the rotational spring constants at  $x = 0$  and  $a$  ( $y = 0$  and  $b$ ), respectively. Eqs. (7)–(14) represent a set of general boundary conditions from which, for example, all the classical homogeneous

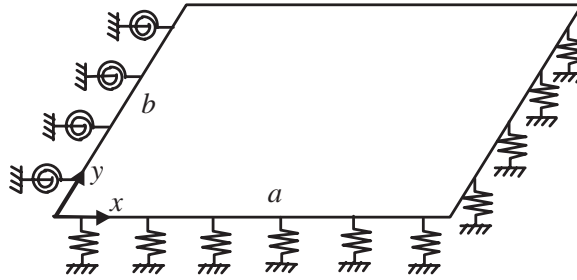


Fig. 1. A rectangular plate elastically restrained along edges.

boundary conditions can be directly obtained by accordingly setting the spring constants equal to an extremely large or small number (see Fig. 1).

An exact solution is normally not available for plates under general boundary conditions, Eqs. (7)–(14). Consequently, the Rayleigh–Ritz method has been widely used to find an approximate solution from Hamilton’s equation

$$\delta \int_{t_0}^{t_1} (T - V) dt = 0, \tag{15}$$

where  $T$  is the total kinetic energy and  $V$  is the total potential energy.

For a purely bending plate, the total potential energy can be expressed as

$$\begin{aligned} V = & \frac{D}{2} \int_0^a \int_0^b \left[ (\partial^2 w / \partial x^2)^2 + (\partial^2 w / \partial y^2)^2 + 2\nu \partial^2 w / \partial x^2 \partial^2 w / \partial y^2 + 2(1 - \nu) (\partial^2 w / \partial x \partial y)^2 \right] dx dy \\ & + \frac{1}{2} \int_0^b \left[ k_{x0} w^2 + K_{x0} (\partial w / \partial x)^2 \right]_{x=0} dy + \frac{1}{2} \int_0^b \left[ k_{x1} w^2 + K_{x1} (\partial w / \partial x)^2 \right]_{x=a} dy \\ & + \frac{1}{2} \int_0^a \left[ k_{y0} w^2 + K_{y0} (\partial w / \partial y)^2 \right]_{y=0} dx + \frac{1}{2} \int_0^a \left[ k_{y1} w^2 + K_{y1} (\partial w / \partial y)^2 \right]_{y=b} dx \end{aligned} \tag{16}$$

and the total kinetic energy is calculated from

$$T = \frac{1}{2} \int_0^a \int_0^b \rho h (\partial w / \partial t)^2 dx dy. \tag{17}$$

In Eq. (16), the first integral represents the strain energy due to the bending of the plate and the rest integrals represent the potential energies stored in the springs.

By substituting Eqs. (16) and (17) into Eq. (15) and integrating by parts, one is able to verify that Eq. (1) and Eqs. (7)–(14) can be actually derived from Eq. (15). It is well known that when the admissible functions form a complete set, the Rayleigh–Ritz solution will converge to the original (boundary value problem) solution.

### 3. Admissible functions

Admissible functions play a critical role in the Rayleigh–Ritz method. For plate problems, the products of the beam functions are often chosen as the admissible functions and the displacement

function can be accordingly expressed as

$$w(x, y) = \sum_{m,n=1} A_{mn} X_m(x) Y_n(y), \tag{18}$$

where  $X_m(x)$  and  $Y_m(y)$  are the characteristic functions for beams that have the same boundary conditions in the  $x$ - and  $y$ -direction, respectively.

Although beam functions can be generally obtained as a linear combination of trigonometric and hyperbolic functions, they include some unknown parameters that have to be determined from the boundary conditions. Consequently, each boundary condition basically leads to a different set of beam functions. In real applications, this is clearly inconvenient, not to mention the tediousness of determining the characteristic functions for a generally supported beam.

In order to avoid this difficulty, an improved Fourier series method have been proposed for beams with arbitrary supports at both ends in which the characteristic functions are sought in the form of [21]:

$$W(x) = \sum_{m=0}^{\infty} a_m \cos \lambda_{am} x + p(x) \quad (\lambda_{am} = m\pi/a), \quad 0 \leq x \leq a. \tag{19}$$

The function  $p(x)$  in Eq. (19) represents an arbitrary continuous function that, regardless of boundary conditions, is always chosen to satisfy the following equations:

$$p'''(0) = W'''(0) = \alpha_0, \quad p'''(a) = W'''(a) = \alpha_1, \tag{20, 21}$$

$$p'(0) = W'(0) = \beta_0 \quad \text{and} \quad p'(a) = W'(a) = \beta_1. \tag{22, 23}$$

As explained in Ref. [21], the function  $p(x)$  is here introduced to take care of the potential discontinuities of the (original) displacement function and its derivatives at the end points. Accordingly, the Fourier series now simply represents a residual displacement function,  $\bar{W}(x) = W(x) - p(x)$ , that is periodic continuous and has at least three continuous derivatives over the entire  $x$ -axis. Mathematically, it is already known that the smoother a periodic function is, the faster its Fourier expansion converges. Therefore, the addition of the function  $p(x)$  will have two immediate benefits: (1) the Fourier series expansion is now applicable to any boundary conditions, and (2) the Fourier series solution can be drastically improved regarding its accuracy convergence.

So far,  $p(x)$  has only been understood as a continuous function that satisfies Eqs. (20)–(23), its form is not a concern with respect to the convergence of the series solution. Thus, the function  $p(x)$  can be selected in any desired form. As a demonstration, suppose that  $p(x)$  is a polynomial function

$$p(x) = \sum_{n=0}^4 c_n P_n(x/a), \tag{24}$$

where  $c_n$  is the expansion coefficient and  $P_n(x)$  is the Legendre function of order  $n$ .

It is obvious that the function  $p(x)$  needs to be at least a fourth order polynomial to simultaneously satisfy Eqs. (20)–(23).

Substituting Eq. (24) into Eqs. (20)–(23) results in

$$c_3 P_3'''(0) + c_4 P_4'''(0) = a^3 \alpha_0, \quad (25)$$

$$c_3 P_3'''(1) + c_4 P_4'''(1) = a^3 \alpha_1, \quad (26)$$

$$c_1 P_1'(0) + c_2 P_2'(0) + c_3 P_3'(0) + c_4 P_4'(0) = a \beta_0, \quad (27)$$

$$c_1 P_1'(1) + c_2 P_2'(1) + c_3 P_3'(1) + c_4 P_4'(1) = a \beta_1. \quad (28)$$

From the above equations, the coefficients,  $c_n$  ( $n = 1, 2, 3, 4$ ), are directly obtainable in terms of the boundary constants,  $\alpha_0, \alpha_1, \beta_0$ , and  $\beta_1$ . Since the constant  $c_0$  does not actually appear in Eqs. (25)–(28), it can be an arbitrary number theoretically. For instance,  $c_0$  is here selected to satisfy

$$\int_0^a p(x) dx = 0. \quad (29)$$

Although Eq. (29) is not necessary, one can verify that it will lead to simplifications of Eqs. (42) and (43).

The final expression for the function  $p(x)$  can be written as

$$p(x) = \zeta_a(x)^T \bar{\alpha}, \quad (30)$$

where

$$\bar{\alpha} = \{\alpha_0, \alpha_1, \beta_0, \beta_1\}^T \quad (31)$$

and

$$\zeta_a(x)^T = \left\{ \begin{array}{l} -(15x^4 - 60ax^3 + 60a^2x^2 - 8a^4)/360a \\ (15x^4 - 30a^2x^2 + 7a^4)/360a \\ (6ax - 2a^2 - 3x^2)/6a \\ (3x^2 - a^2)/6a \end{array} \right\}. \quad (32)$$

The results in Eqs. (30)–(32) were previously derived from a more straightforward but less general approach in Ref. [21].

In order to determine the unknown boundary constants,  $\alpha_0, \alpha_1, \beta_0$ , and  $\beta_1$ , substitution of Eqs. (19) and (30) into the boundary conditions Eqs. (7)–(14) results in

$$\bar{\alpha} = \sum_{m=0}^{\infty} \mathbf{H}_a^{-1} \mathbf{Q}_{am} a_m, \quad (33)$$

where

$$\mathbf{H}_a = \begin{bmatrix} \frac{8\hat{k}_{x0}a^3}{360} + 1 & \frac{7\hat{k}_{x0}a^3}{360} & \frac{-\hat{k}_{x0}a}{3} & \frac{-\hat{k}_{x0}a}{6} \\ \frac{7\hat{k}_{x1}a^3}{360} & \frac{8\hat{k}_{x1}a^3}{360} + 1 & \frac{-\hat{k}_{x1}a}{6} & \frac{-\hat{k}_{x1}a}{3} \\ \frac{a}{3} & \frac{a}{6} & \hat{K}_{x0} + \frac{1}{a} & \frac{-1}{a} \\ \frac{a}{6} & \frac{a}{3} & \frac{-1}{a} & \hat{K}_{x1} + \frac{1}{a} \end{bmatrix} \quad (34)$$

and

$$\mathbf{Q}_{am} = \left\{ -\hat{k}_{x0} \quad (-1)^m \hat{k}_{x1} \quad -\lambda_{am}^2 \quad (-1)^m \lambda_{am}^2 \right\}^T. \tag{35}$$

It should be mentioned that the matrix  $\mathbf{H}_a$  will become singular for a completely free beam. However, this problem can be overcome to a certain extent by artificially attaching one or more springs with very small stiffnesses to the ends of a beam. It has been shown in Ref. [25] that although the matrix may be ill-conditioned in such a treatment, the natural frequencies can still be accurately calculated for a completely free beam. Nevertheless, the characteristic functions are well known for this particular case and can be readily used as the admissible functions in the Rayleigh–Ritz method.

Making use of Eqs. (30) and (33), Eq. (19) can be rewritten as

$$W(x) = \sum_{m=0}^{\infty} a_m \psi_m^a(x), \tag{36}$$

where

$$\psi_m^a(x) = \sqrt{2/a} (\cos \lambda_{am}x + \zeta_a(x)^T \mathbf{H}_a^{-1} \mathbf{Q}_{am}). \tag{37}$$

Mathematically, Eq. (36) indicates that each of the beam functions can be viewed as a function in the functional space spanned by the basis functions  $\{\psi_m^a(x); m = 0, 1, 2, \dots\}$ . Thus, Eq. (18) can be accordingly rewritten as

$$w(x, y) = \sum_{m,n=0}^{\infty} A_{mn} \psi_m^a(x) \psi_n^b(y), \tag{38}$$

where

$$\psi_n^b(y) = \sqrt{2/b} (\cos \lambda_{bn}y + \zeta_b(y)^T \mathbf{H}_b^{-1} \mathbf{Q}_{bn}). \tag{39}$$

The expressions for  $\zeta_b(y)$ ,  $\mathbf{H}_b$  and  $\mathbf{Q}_{bn}$  can be, respectively, obtained from Eqs. (32), (34) and (35) by simply replacing the  $x$ -related parameters by the  $y$ -related.

By substituting Eqs. (16), (17) and (38) into Eq. (15), one will have

$$(\mathbf{K} - \rho_D \omega^2 \mathbf{M}) \mathbf{A} = \mathbf{0}, \tag{40}$$

where

$$\mathbf{A} = \{A_{00}, A_{01}, \dots, A_{m0}, A_{m1}, \dots, A_{mn}, \dots\}^T, \tag{41}$$

$$\begin{aligned} K_{mn,m'n'} = & (\lambda_{am}^2 \lambda_{am'}^2 \varepsilon_m \delta_{mm'} - \lambda_{am}^2 \bar{S}_{mm'}^a - \lambda_{am'}^2 \bar{S}_{m'm}^a + \bar{Z}_{mm'}^a) (\varepsilon_n \delta_{nn'} + S_{nn'}^b + S_{n'n}^b + Z_{nn'}^b) \\ & + (\varepsilon_m \delta_{mm'} + S_{mm'}^a + S_{m'm}^a + Z_{mm'}^a) (\lambda_{bn}^2 \lambda_{bn'}^2 \varepsilon_n \delta_{nn'} - \lambda_{bn}^2 \bar{S}_{nn'}^b - \lambda_{bn'}^2 \bar{S}_{n'n}^b + \bar{Z}_{nn'}^b) \\ & + \nu (-\lambda_{am}^2 \varepsilon_m \delta_{mm'} - \lambda_{am'}^2 S_{mm'}^a + \bar{S}_{m'm}^a + \hat{Z}_{mm'}^a) (-\lambda_{bn}^2 \varepsilon_n \delta_{nn'} - \lambda_{bn'}^2 S_{nn'}^b + \bar{S}_{nn'}^b + \hat{Z}_{n'n}^b) \\ & + \nu (-\lambda_{am'}^2 \varepsilon_m \delta_{mm'} - \lambda_{am}^2 S_{m'm}^a + \bar{S}_{mm'}^a + \hat{Z}_{m'm}^a) (-\lambda_{bn}^2 \varepsilon_n \delta_{nn'} - \lambda_{bn'}^2 S_{nn'}^b + \bar{S}_{n'n}^b + \hat{Z}_{nn'}^b) \\ & + 2(1 - \nu) (\lambda_{am} \lambda_{am'} \varepsilon_m \delta_{mm'} - \lambda_{am} \bar{S}_{mm'}^a - \lambda_{am'} \bar{S}_{m'm}^a + \bar{Z}_{mm'}^a) \\ & \times (\lambda_{bn} \lambda_{bn'} \varepsilon_n \delta_{nn'} - \lambda_{bn} \bar{S}_{nn'}^b - \lambda_{bn'} \bar{S}_{n'n}^b + \bar{Z}_{nn'}^b) \\ & + (\hat{k}_{x0} \psi_m^a(0) \psi_{m'}^a(0) + \hat{K}_{x0} \psi_{xm}^a(0) \psi_{xm'}^a(0)) (\varepsilon_n \delta_{nn'} + S_{nn'}^b + S_{n'n}^b + Z_{nn'}^b) \end{aligned}$$

$$\begin{aligned}
 &+ (\hat{K}_{x1}\psi_m^a(a)\psi_{m'}^a(a) + \hat{K}_{x1}\psi_{xm}^a(a)\psi_{xm'}^a(a))(\varepsilon_n\delta_{nn'} + S_{nn'}^b + S_{n'n}^b + Z_{nn'}^b) \\
 &+ (\hat{K}_{y0}\psi_n^b(0)\psi_{n'}^b(0) + \hat{K}_{y0}\psi_{yn}^b(0)\psi_{yn'}^b(0))(\varepsilon_m\delta_{mm'} + S_{mm'}^a + S_{m'm}^a + Z_{mm'}^a) \\
 &+ (\hat{K}_{y1}\psi_n^b(b)\psi_{n'}^b(b) + \hat{K}_{y1}\psi_{yn}^b(b)\psi_{yn'}^b(b))(\varepsilon_m\delta_{mm'} + S_{mm'}^a + S_{m'm}^a + Z_{mm'}^a)
 \end{aligned} \tag{42}$$

and

$$M_{mn,m'n'} = (\varepsilon_m\delta_{mm'} + S_{mm'}^a + S_{m'm}^a + Z_{mm'}^a)(\varepsilon_n\delta_{nn'} + S_{nn'}^b + S_{n'n}^b + Z_{nn'}^b). \tag{43}$$

For conciseness, the definitions or expressions for all the new symbols in Eq. (42) are given later in Appendix B.

In deriving Eq. (40), the functions  $\psi_m^a(x)\psi_n^b(y)$ ,  $m, n = 0, 1, 2, \dots$ , have been used as a set of admissible functions. The completeness of the functions  $\psi_m^a(x)$ ,  $m = 0, 1, 2, \dots$ , (also,  $\psi_m^a(x)\psi_n^b(y)$ ) can be readily established from that of the cosine functions. Mathematically, the completeness of the admissible functions ensures that the resulting Rayleigh–Ritz solution will be always convergent.

It should be pointed out that although the auxiliary function  $p(x)$  is here specifically sought as a polynomial, it can actually be any other continuous function defined over  $[0, a]$ . In such a case,  $P_n(x)$  may be simply understood as a set of given functions and one can still follow the above procedure to find the relationship between the expansion coefficients  $c_n(x)$  and the boundary constants  $\alpha_0, \alpha_1, \beta_0$ , and  $\beta_1$ .

#### 4. Results and discussions

Several example problems involving various boundary conditions will be solved in this section. First, consider a plate clamped along all edges. A clamped edge can be viewed as a special case when the stiffnesses for the (translational and rotational) boundary springs become infinitely large (which is actually represented by a very large number, 1.0E + 10, in the following numerical calculations). In Table 1, the first six frequency parameters,  $\Omega = \omega a^2 \sqrt{\rho h/D}$ , are shown for the plates of different aspect ratios. The results compare well with those previously obtained from the characteristic functions for a clamped beam. It is obvious that in numerical calculations Eq. (40)

Table 1  
Frequency parameters,  $\Omega = \omega a^2 \sqrt{\rho h/D}$ , for C-C-C-C plates of different aspect ratios

$a/b$	$\Omega = \omega a^2 \sqrt{\rho h/D}$					
	1	2	3	4	5	6
1.0	35.99 (35.99 <sup>a</sup> )	73.40 (73.41)	73.40 (73.41)	108.2 (108.3)	131.6 (131.6)	132.2 (132.2)
1.5	60.76	93.84	148.8	149.7	179.6	226.8
2.0	98.31	127.3	179.1	253.3	255.9	284.3
2.5	147.8	173.8	221.4	291.7	384.4	394.3

<sup>a</sup> Note: results in parentheses are taken from Ref. [26, p. 261].



has to be truncated to the first  $(M + 1) \times (N + 1)$  terms corresponding to  $m = 0, 1, 2, \dots, M$  and  $n = 0, 1, 2, \dots, N$ . Specifically, the frequency parameters in Table 1 are determined by setting  $M = N = 6$ . To check the convergence of the solution, Table 2 gives the frequencies (for  $b/a = 1$ ) calculated using different numbers of terms (that is,  $M = N = 3, 4, 5, 6, 7$ ). The convergence of the solutions for other cases or boundary conditions can be examined in the same way. For the sake of conciseness, however, the displacement expansion, Eq. (38), will be simply truncated to  $M = N = 6$  in the subsequent calculations.

Table 2  
Frequency parameters,  $\Omega = \omega a^2 \sqrt{\rho h / D}$ , for a C-C-C-C square plate

$M = N$	$\Omega = \omega a^2 \sqrt{\rho h / D}$					
	1	2	3	4	5	6
3	35.991	73.410	73.410	108.24	134.50	135.22
4	35.986	73.398	73.398	108.24	131.59	132.22
5	35.986	73.397	73.397	108.22	131.59	132.22
6	35.986	73.395	73.395	108.22	131.58	132.21
7	35.986	73.395	73.395	108.22	131.58	132.21

Table 3  
Frequency parameters,  $\Omega = \omega a^2 \sqrt{\rho h / D}$ , for C-S-S-F plates of different aspect ratios

$a/b$	$\Omega = \omega a^2 \sqrt{\rho h / D}$					
	1	2	3	4	5	6
1.0	16.87 (16.87 <sup>a</sup> )	31.14 (31.14)	51.64 (51.63)	64.03 (64.04)	67.64 (67.65)	101.2 (101.2)
1.5	18.54	50.43	53.72	88.78	108.2	126.1
2.0	20.65	56.54	77.33	111.3	117.3	176.0
2.5	23.07	59.97	111.9	115.1	153.1	189.6

<sup>a</sup> Note: results in parentheses are taken from Ref. [26, p. 257].

Table 4  
Frequency parameters,  $\Omega = \omega a^2 \sqrt{\rho h / D}$ , for S-S-F-F plates of different aspect ratios

$a/b$	$\Omega = \omega a^2 \sqrt{\rho h / D}$					
	1	2	3	4	5	6
1.0	3.369 (3.369 <sup>a</sup> )	17.41 (17.41)	19.37 (19.37)	38.30 (38.29)	51.35 (51.32)	53.74 (53.74)
1.5	5.026	21.55	37.73	55.50	60.89	99.40
2.0	6.647	25.46	59.05	65.51	89.34	113.8
2.5	8.251	29.65	64.77	99.24	118.3	126.1

<sup>a</sup> Note: results in parentheses are taken from Ref. [26, p. 254].

The next example also deals with a classical case: a plate clamped along  $x = 0$ , simply supported along  $y = 0$  and  $x = a$ , and free at  $y = b$ . The simply supported edge condition is created by simply setting the stiffnesses of the translational and rotational springs to  $\infty$  and 0, respectively. The free edge condition is obtained by setting both stiffnesses to zero. The six smallest frequency parameters,  $\Omega = \omega a^2 \sqrt{\rho h / D}$ , are given in Table 3 for various plate aspect ratios.

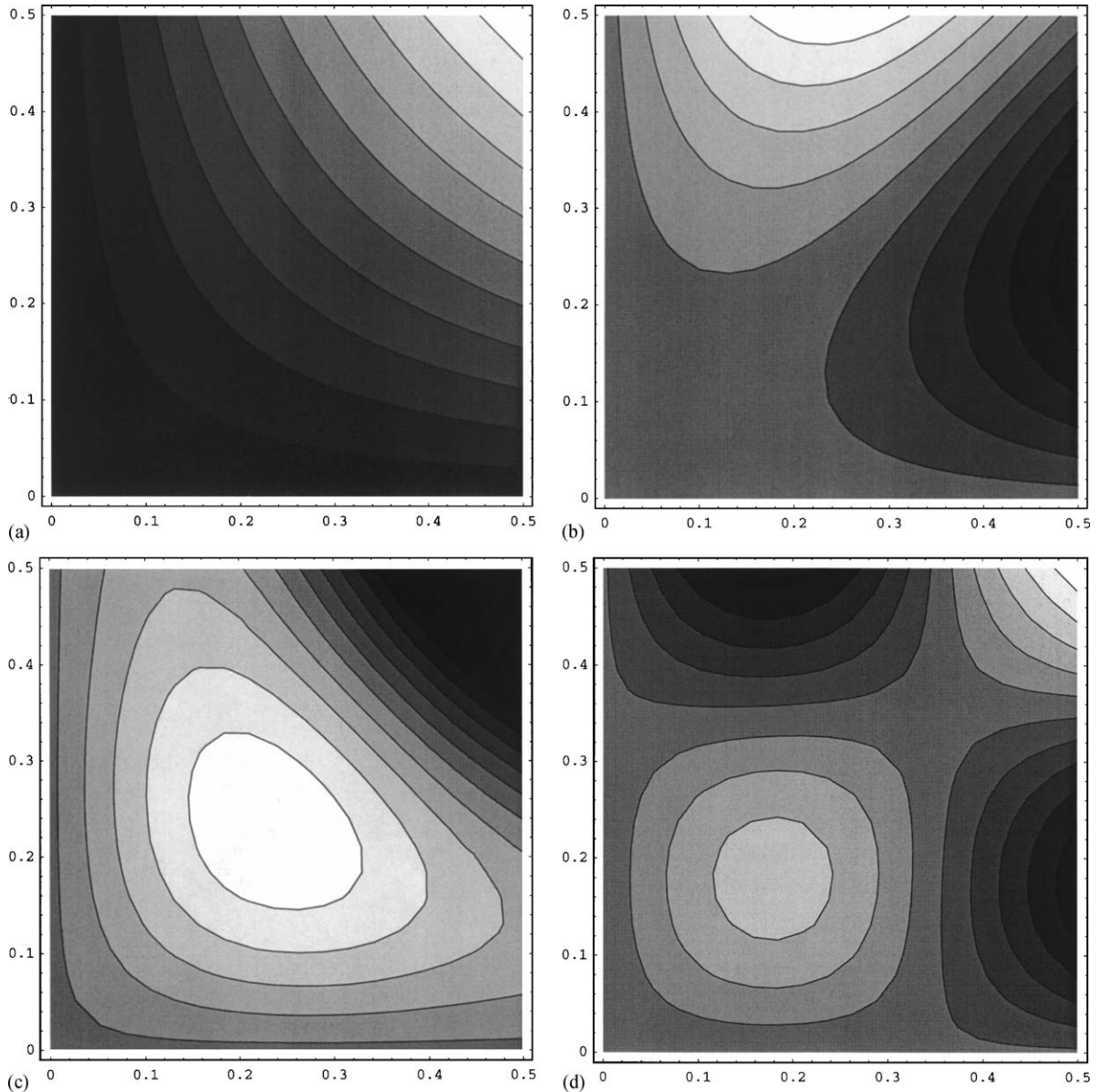


Fig. 2. The mode shapes for an S-S-F-F square plate: (a) the first mode; (b) second; (c) third; (d) fourth; (e) fifth; and (f) sixth.

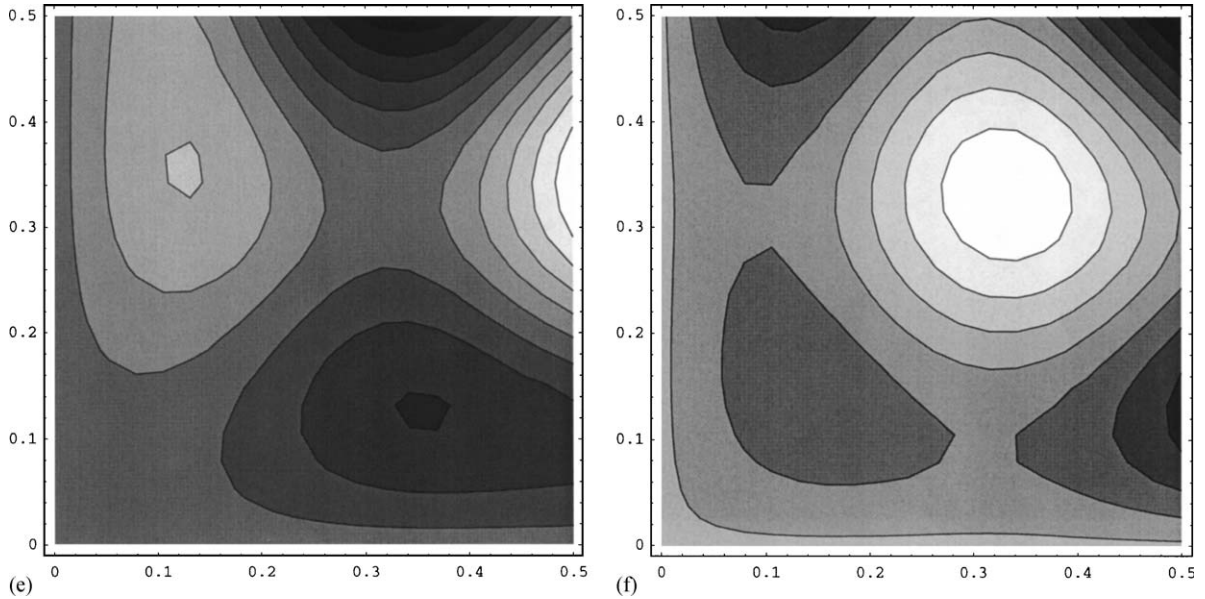


Fig. 2 (continued).

Before proceeding to elastically restrained plates, one more classical homogeneous boundary condition will be considered: simply supported at  $x = 0$  and  $y = 0$  and free along the other edges. Unlike in the two previous boundary conditions, the plate is now allowed to move freely at one of its corners. This implies that an additional twist-free condition has been implicitly imposed upon the variational solution at that corner. The lowest frequency parameters are listed in Table 4. For any given frequency parameter, its corresponding mode shape can be readily determined from Eq. (38). For example, the first six mode shapes of the square plate are plotted in Fig. 2.

Let us now consider two more complicated problems in which plates are elastically restrained along edges. The first one involves a simply supported square plate with a uniform elastic restraint against rotation along each edge, that is,  $\hat{K}_{x0}a = \hat{K}_{x1}a = \hat{K}_{y0}a = \hat{K}_{y1}a = \hat{K}a$ . In Table 5, the first six frequency parameters are shown for a few different stiffness values. For comparison, the previous results for  $\hat{K}a = 20$  are also given there. Because of the symmetries about the  $x$ - and  $y$ -axis, the second and third frequency parameters are identical. The fifth and sixth frequency parameters are also the same for  $\hat{K}a = 0$ . However, they become slightly different for other stiffness values. It should be noted that this is not caused by the numerical errors. As a matter of fact, they represent two closely spaced, but substantially different, modes as shown in Fig. 3.

Finally, consider a square plate clamped along  $x = 0$  and elastically restrained against deflection at  $x = a$  and against rotation at  $y = a$ . Given in Tables 6 and 7 are the lowest frequency parameters for various combinations of the translational and rotational springs. It is observed that in this example the lowest frequency is barely affected by the stiffness of the rotational spring. In comparison, the rotational spring has more impacts on the fourth and higher order modes. To better understand this, the mode shapes of the first and fourth modes are plotted in Fig. 4 for  $\hat{k}_{x1}a^3 = 10$  and  $\hat{K}_{y1}a = 1$ . It is seen that for the first mode the slope or gradient in the  $y$ -direction is

Table 5

The frequency parameters,  $\Omega = \omega a^2 \sqrt{\rho h/D}$ , for an S-S-S-S square plate with uniform rotational restraint along edges

$\hat{K}a$	$\Omega = \omega a^2 \sqrt{\rho h/D}$					
	1	2	3	4	5	6
0	19.74	49.35	49.35	78.96	98.70	98.70
10	28.50	60.22	60.22	90.81	111.2	111.4
20	31.08 (31.09 <sup>a</sup> )	64.31 (64.31)	64.31 (64.31)	95.82 (95.85)	116.8 (116.8)	117.2 (117.3)
100	34.67	70.78	70.78	104.5	127.0	127.6
$\infty$	35.99	73.40	73.40	108.2	131.6	132.2

<sup>a</sup> Note: results in parentheses are taken from Ref. [1, p. 124].

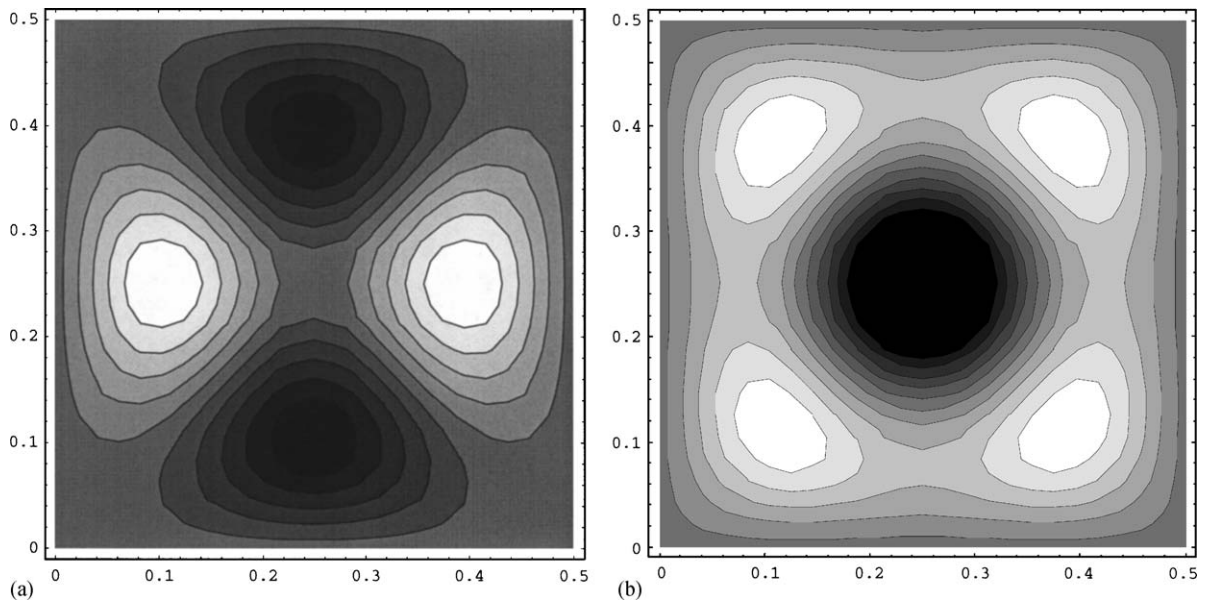


Fig. 3. The mode shapes for a simply supported square plate with a uniform rotational restraint,  $\hat{K}a = 10$ , along each edge: (a) the fifth mode; (b) the sixth mode.

Table 6

The frequency parameters,  $\Omega = \omega a^2 \sqrt{\rho h/D}$ , for a C-F-F-F square plate with translational and rotational restraints at  $x = a$  and  $y = a$ , respectively.  $\hat{k}_{x1} a^3 = 10$

$\hat{K}_{b1} a$	$\Omega = \omega a^2 \sqrt{\rho h/D}$					
	1	2	3	4	5	6
1	6.957	10.46	22.54	28.92	31.95	55.219
10	6.959	11.26	22.79	31.62	32.96	57.06
100	6.960	11.54	22.85	32.16	34.34	58.30

Table 7

The frequency parameters,  $\Omega = \omega a^2 \sqrt{\rho h/D}$ , for a C-F-F-F square plate with translational and rotational restraints at  $x = a$  and  $y = a$ , respectively.  $\hat{k}_{x1} a^3 = 100$

$\hat{K}_{b1} a$	$\Omega = \omega a^2 \sqrt{\rho h/D}$					
	1	2	3	4	5	6
1	13.15	16.12	30.98	32.32	37.67	57.97
10	13.18	16.82	31.42	35.18	38.05	59.78
100	13.18	17.08	31.46	36.77	38.31	61.01

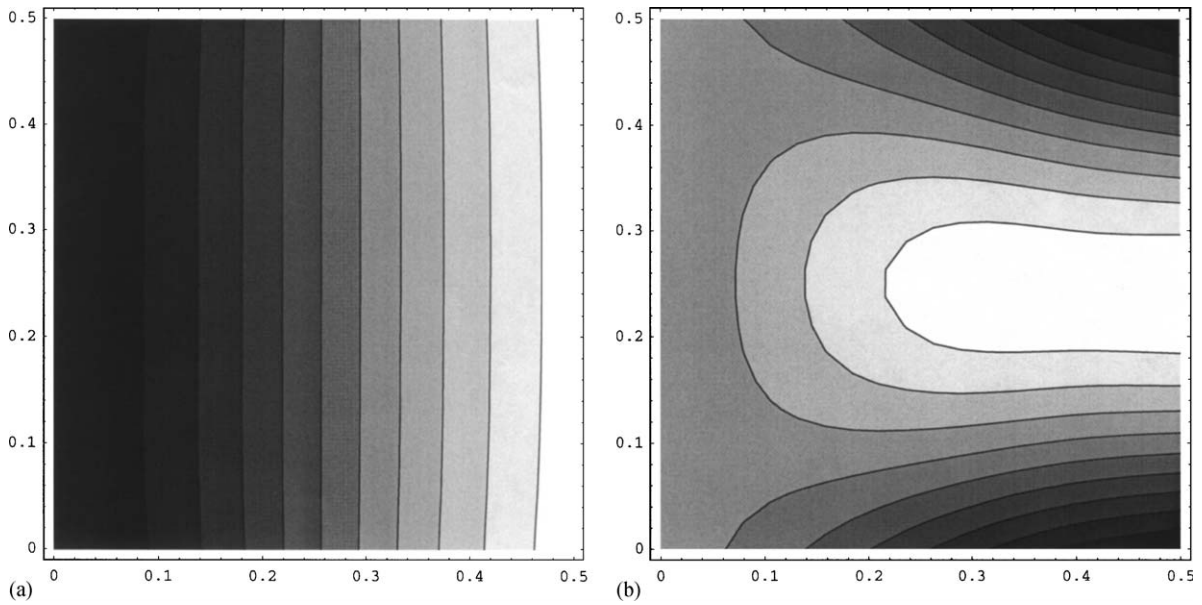


Fig. 4. The mode shapes for a C-F-F-F square plate elastically restrained against deflection at  $x = a$  and against rotation at  $y = a$ .  $\hat{k}_{x1} a^3 = 10$  and  $\hat{K}_{y1} a = 1$ : (a) the first mode; (b) the fourth mode.

so small that the rotational spring is essentially not loaded by the plate and vice versa. This is obviously not the case for the fourth mode.

### 5. Conclusions

A new set of admissible functions has been used in the Rayleigh–Ritz method for the free vibrations of rectangular plates with general elastic restraints along the edges. Each of these admissible functions is expressed as a trigonometric function plus a polynomial function. The polynomials are included here only to overcome the potential discontinuity problem of the

displacement function at the edges when it is periodically extended onto the entire  $x$ – $y$  plane. The remarkable convergence and accuracy of the current solution have been repeatedly demonstrated through the numerical examples.

Although in the above discussion polynomial functions have been specifically used to supplement the trigonometric functions, any other continuous functions should be equally applicable in that regard. Therefore, this investigation has actually developed a general technique for deriving a complete set of admissible functions that can be universally applied to various boundary conditions including the more complicated elastic boundary supports.

## Appendix A. Nomenclature

<b>A</b>	vector of the expansion or Rayleigh–Ritz coefficients
$A_{mn}$	expansion or Rayleigh–Ritz coefficients
$a$	length of a plate
$a_m$	expansion or Rayleigh–Ritz coefficient
$b$	width of a plate
$D$	flexural rigidity
$h$	plate thickness
<b>K</b>	stiffness matrix
$K_{x0}, K_{x1}$	rotational stiffnesses at $x = 0$ and $a$ , respectively
$K_{y0}, K_{y1}$	rotational stiffnesses at $y = 0$ and $b$ , respectively
$\hat{K}_{x0}, \hat{K}_{x1}$	(= $K_{x0}/D, K_{x1}/D$ )
$\hat{K}_{y0}, \hat{K}_{y1}$	(= $K_{y0}/D, K_{y1}/D$ )
$k_{x0}, k_{x1}$	translational stiffnesses at $x = 0$ and $a$ , respectively
$k_{y0}, k_{y1}$	translational stiffnesses at $y = 0$ and $b$ , respectively
$\hat{k}_{x0}, \hat{k}_{x1}$	(= $k_{x0}/D, k_{x1}/D$ )
$\hat{k}_{y0}, \hat{k}_{y1}$	(= $k_{y0}/D, k_{y1}/D$ )
<b>M</b>	mass matrix
$M, N$	numbers of expansion terms used in $x$ - and $y$ -direction, respectively
$M_x, M_y$	bending moments
$M_{xy}$	twisting moment
$p(x)$	a simple polynomial function
$Q_x, Q_y$	shear forces
$T$	kinetic energy
$U$	strain energy
$W(x)$	flexural displacement of a beam
$w(x, y)$	flexural displacement of a plate
$X_m(x)$	beam characteristic function
$Y_n(y)$	beam characteristic function
$\alpha_0, \alpha_1$	(= $W'''(0), W'''(a)$ )
$\beta_0, \beta_1$	(= $W'(0), W'(a)$ )
$\delta_{mn}$	Kronecker delta function

- $\varepsilon_m$       ( $= (1 + \delta_{m0})$ )
- $\lambda_{am}$      ( $= \frac{m\pi}{a}$ )
- $\lambda_{bn}$      ( $= \frac{n\pi}{b}$ )
- $\Omega$         ( $= \omega a^2 \sqrt{\rho h/D}$ )
- $\rho$         mass density
- $\omega$         frequency in radian
- $\psi_m^a(x)$     admissible functions in  $x$ -direction
- $\psi_n^b(y)$     admissible functions in  $y$ -direction

**Appendix B. Supplementary definitions**

The new symbols, vectors and matrices in Eq. (42) are defined as follows:

$$S_{mm'}^\alpha = \mathbf{P}_{\alpha m}^\top \mathbf{H}_\alpha^{-1} \mathbf{Q}_{\alpha m'}, \quad \bar{S}_{mm'}^\alpha = \bar{\mathbf{P}}_{\alpha m}^\top \mathbf{H}_\alpha^{-1} \mathbf{Q}_{\alpha m'} \quad (\alpha = a, b), \tag{B.1, B.2}$$

$$\bar{S}_{mm'}^\alpha = \bar{\mathbf{P}}_{\alpha m}^\top \mathbf{H}_\alpha^{-1} \mathbf{Q}_{\alpha m'}, \quad Z_{mm'}^\alpha = \mathbf{Q}_{\alpha m}^\top \mathbf{H}_\alpha^{-\top} \bar{\boldsymbol{\Xi}}_\alpha \mathbf{H}_\alpha^{-1} \mathbf{Q}_{\alpha m'}, \tag{B.3, B.4}$$

$$\bar{Z}_{mm'}^\alpha = \mathbf{Q}_{\alpha m}^\top \mathbf{H}_\alpha^{-\top} \bar{\bar{\boldsymbol{\Xi}}}_\alpha \mathbf{H}_\alpha^{-1} \mathbf{Q}_{\alpha m'}, \quad \bar{\bar{Z}}_{mm'}^\alpha = \mathbf{Q}_{\alpha m}^\top \mathbf{H}_\alpha^{-\top} \bar{\bar{\boldsymbol{\Xi}}}_\alpha \mathbf{H}_\alpha^{-1} \mathbf{Q}_{\alpha m'}, \tag{B.5, B.6}$$

$$\hat{Z}_{mm'}^\alpha = \mathbf{Q}_{\alpha m}^\top \mathbf{H}_\alpha^{-\top} \hat{\boldsymbol{\Xi}}_\alpha \mathbf{H}_\alpha^{-1} \mathbf{Q}_{\alpha m'} \tag{B.7}$$

and

$$\varepsilon_m = (1 + \delta_{m0}) \tag{B.8}$$

with

$$\begin{aligned} \mathbf{P}_{am} &= \int_0^a \zeta(x) \cos \lambda_{am}x \, dx \\ &= \begin{cases} \{0 \ 0 \ 0 \ 0\}^\top, & \text{for } m = 0, \\ \left\{ \frac{1}{\lambda_{am}^4} \frac{(-1)^{m+1}}{\lambda_{am}^4} \frac{-1}{\lambda_{am}^2} \frac{(-1)^m}{\lambda_{am}^2} \right\}^\top, & \text{for } m \neq 0, \end{cases} \end{aligned} \tag{B.9}$$

$$\begin{aligned} \bar{\mathbf{P}}_{am} &= \int_0^a \zeta'(x) \sin \lambda_{am}x \, dx, \\ &= \begin{cases} \{0 \ 0 \ 0 \ 0\}^\top, & \text{for } m = 0, \\ \left\{ \frac{-1}{\lambda_{am}^3} \frac{(-1)^m}{\lambda_{am}^3} \frac{1}{\lambda_{am}} \frac{(-1)^{m+1}}{\lambda_{am}} \right\}^\top, & \text{for } m \neq 0, \end{cases} \end{aligned} \tag{B.10}$$

$$\begin{aligned} \bar{\mathbf{P}}_{am} &= \int_0^a \zeta''(x) \cos \lambda_{am} x \, dx \\ &= \begin{cases} \{0 \ 0 \ -1 \ 1\}^T, & \text{for } m = 0, \\ \left\{ \frac{-1}{\lambda_{am}^2} \frac{(-1)^m}{\lambda_{am}^2} \ 0 \ 0 \right\}^T, & \text{for } m \neq 0, \end{cases} \end{aligned} \tag{B.11}$$

$$\bar{\mathbf{E}} = \int_0^a \zeta_a(x)^T \zeta_a(x) \, dx = \begin{bmatrix} \frac{a^7}{4725} & & & & \\ \frac{127a^6}{604800} & \frac{a^7}{4725} & \text{sym.} & & \\ -\frac{2a^5}{945} & -\frac{31a^5}{15120} & \frac{a^3}{45} & & \\ \frac{31a^5}{15120} & -\frac{2a^5}{945} & \frac{7a^3}{360} & \frac{a^3}{45} & \\ -\frac{2a^5}{945} & \frac{31a^5}{15120} & \frac{a^3}{45} & \frac{a^3}{45} & \end{bmatrix}, \tag{B.12}$$

$$\bar{\mathbf{E}}^{\text{I}} = \int_0^a \zeta'_a(x)^T \zeta'_a(x) \, dx = \begin{bmatrix} \frac{2a^5}{945} & & & & \\ \frac{31a^5}{15120} & \frac{2a^5}{945} & \text{sym.} & & \\ -\frac{a^3}{45} & -\frac{7a^3}{360} & \frac{a}{3} & & \\ \frac{7a^3}{360} & -\frac{a^3}{45} & \frac{a}{6} & \frac{a}{3} & \\ -\frac{a^3}{45} & \frac{7a^3}{360} & \frac{a}{3} & \frac{a}{3} & \end{bmatrix}, \tag{B.13}$$

$$\bar{\mathbf{E}}^{\text{II}} = \int_0^a \zeta''_a(x)^T \zeta''_a(x) \, dx = \begin{bmatrix} \frac{a^3}{45} & & & & \\ \frac{7a^3}{360} & \frac{a^3}{45} & \text{sym.} & & \\ 0 & 0 & \frac{1}{a} & & \\ 0 & 0 & -\frac{1}{a} & \frac{1}{a} & \\ 0 & 0 & \frac{1}{a} & -\frac{1}{a} & \end{bmatrix} \tag{B.14}$$

and

$$\hat{\mathbf{E}} = \int_0^a \zeta''_a(x)^T \zeta_a(x) \, dx = \begin{bmatrix} -\frac{2a^5}{945} & -\frac{31a^5}{15120} & \frac{a^3}{45} & \frac{7a^3}{360} \\ -\frac{31a^5}{15120} & -\frac{2a^5}{945} & \frac{7a^3}{360} & \frac{a^3}{45} \\ 0 & 0 & 0 & 0 \\ 0 & 0 & 0 & 0 \end{bmatrix}. \tag{B.15}$$



## References

- [1] A.W. Leissa, *Vibration of Plates*, Acoustical Society of America, 1993.
- [2] G.B. Warburton, The vibrations of rectangular plates, *Proceeding of the Institute of Mechanical Engineers, Series A* 168 (1954) 371–384.
- [3] A.W. Leissa, The free vibrations of rectangular plates, *Journal of Sound and Vibration* 31 (1973) 257–293.
- [4] S.M. Dickinson, E.K.H. Li, On the use of simply supported plate functions in the Rayleigh–Ritz method applied to the vibration of rectangular plates, *Journal of Sound and Vibration* 80 (1982) 292–297.
- [5] G.B. Warburton, Response using the Rayleigh–Ritz method, *Journal of Earthquake Engineering and Structural Dynamics* 7 (1979) 327–334.
- [6] T.E. Carmichael, The vibration of a rectangular plate with edges elastically restrained against rotation, *Quarterly Journal of Mechanics and Applied Mathematics* 12 (1959) 29–42.
- [7] P.A.A. Laura, R.O. Grossi, Transverse vibration of a rectangular plate elastically restrained against rotation along three edges and free on the fourth edge, *Journal of Sound and Vibration* 59 (1978) 355–368.
- [8] G.B. Warburton, S.L. Edney, Vibrations of rectangular plates with elastically restrained edges, *Journal of Sound and Vibration* 95 (1984) 537–552.
- [9] D.J. Gorman, A comprehensive study of the free vibration of rectangular plates resting on symmetrically distributed uniform elastic edge supports, *Journal of Applied Mechanics* 56 (1980) 893–899.
- [10] A.V. Bapat, N. Venkatramani, S. Suryanarayan, Simulation of classical edge conditions by finite elastic restraints in the vibration analysis of plates, *Journal of Sound and Vibration* 120 (1988) 127–140.
- [11] P. Cupial, Calculation of the natural frequencies of composite plates by the Rayleigh–Ritz method with orthogonal polynomials, *Journal of Sound and Vibration* 201 (1997) 385–387.
- [12] R.B. Bhat, Natural frequencies of rectangular plates using characteristic orthogonal polynomials in the Rayleigh–Ritz method, *Journal of Applied Mechanics* 102 (1985) 493–499.
- [13] S.M. Dickinson, A. Di-Blasio, On the use of orthogonal polynomials in the Rayleigh–Ritz method for the flexural vibration and buckling of isotropic and orthotropic rectangular plates, *Journal of Applied Mechanics* 108 (1986) 51–62.
- [14] P.A.A. Laura, Comments on “Natural frequencies of rectangular plates using a set of static beam functions in the Rayleigh–Ritz method”, *Journal of Sound and Vibration* 200 (1997) 540–542.
- [15] C.P. Filipich, M.B. Rosales, Arbitrary precision frequencies of a free rectangular thin plate, *Journal of Sound and Vibration* 230 (2000) 521–539.
- [16] O. Beslin, J. Nicolas, A hierarchical functions sets for very high-order plate bending modes with any boundary conditions, *Journal of Sound and Vibration* 202 (1997) 633–655.
- [17] D. Zhou, Natural frequencies of rectangular plates using a set of static beam functions in the Rayleigh–Ritz method, *Journal of Sound and Vibration* 189 (1996) 81–88.
- [18] S. Hurlebaus, L. Gaul, J.T.-S. Wang, An exact series solution for calculating the natural frequencies of orthotropic plates with completely free boundary, *Journal of Sound and Vibration* 244 (2001) 747–759.
- [19] J.T.-S. Wang, C.-C. Lin, Dynamic analysis of generally supported beams using Fourier series, *Journal of Sound and Vibration* 196 (1996) 285–293.
- [20] R.L. Ramkumar, P.C. Chen, W.J. Sanders, Free vibration solution for clamped orthotropic plates using Lagrangian multiplier technique, *American Institute of Aeronautics and Astronautics* 25 (1987) 146–151.
- [21] W.L. Li, Free vibrations of beams with general boundary conditions, *Journal of Sound and Vibration* 237 (2000) 709–725.
- [22] W.L. Li, Dynamic analysis of beams with arbitrary elastic supports at both ends, *Journal of Sound and Vibration* 246 (2001) 751–756.
- [23] W.L. Li, M. Daniels, A Fourier series method for the vibrations of elastically restrained plates arbitrarily loaded with springs and masses, *Journal of Sound and Vibration* 252 (2002) 768–781.
- [24] W.L. Li, Comparison of Fourier sine and cosine series expansions for beams with arbitrary boundary conditions, *Journal of Sound and Vibration* 255 (2002) 185–194.
- [25] W.L. Li, Reply to: discussion on “free vibrations of beams with general boundary conditions”, *Journal of Sound and Vibration* 257 (2002) 593–595.
- [26] R.D. Blevins, *Formulas for Natural Frequency and Mode Shape*, Van Nostrand Reinhold Company, New York, 1979.